KSME

Springer

Journal of Mechanical Science and Technology 38 (9) 2024

Original Article
DOI 10.1007/s12206-024-2409-6

Keywords:
· Carbonization
· Vitreous carbon grid structure
· 3D printing
· Digital light processing
· Water-oil separation

Correspondence to:
Young Kyu Kim
kykdes@cau.ac.kr;
Seok-min Kim
smkim@cau.ac.kr

Citation:
Kim, J. W., Kim, C., Na, H., Lee, S., Seok, S., Byeon, S., Kim, Y. K., Kim, S.-m. (2024). Fabrication of vitreous carbon grid structures by carbonization of 3D printed parts for water-oil separation. Journal of Mechanical Science and Technology 38 (9) (2024) 4557~4562.
http://doi.org/10.1007/s12206-024-2409-6

Received April 29th, 2024
Revised June 20th, 2024
Accepted June 20th, 2024

† This paper was presented at ICD3DP 2023, Booyoung Hotel & Resort, Jeju Island, Korea, October 18-21, 2023. Recommended by Guest Editor Dong-Gyu Ahn

Fabrication of vitreous carbon grid structures by carbonization of 3D printed parts for water-oil separation

Ju Wan Kim[1,2], Chanwoo Kim[3], Hyunjin Na[3], Seongmin Lee[2], Suyeon Seok[1,2], Seongyong Byeon[2], Young Kyu Kim[1] and Seok-min Kim[1,2,3]

[1]Department of Computer Science and Engineering, Graduate School, Chung-Ang University, 84 Heukseok-ro, Dongjak-gu, Seoul 06974, Korea, [2]Department of Mechanical Engineering, Graduate School, Chung-Ang University, 84 Heukseok-ro, Dongjak-gu, Seoul 06974, Korea, [3]School of Mechanical Engineering, Chung-Ang University, 84 Heukseok-ro, Dongjak-gu, Seoul 06974, Korea

Abstract An effective oil separating technique from water-oil mixture can be used in various industrial fields such as environmental purification and resource recycling. In this study, a vitreous carbon (VC) grid structure was fabricated by carbonization of digital light processing (DLP) 3D (3-dimensional) printed parts, and its oil separation performance was evaluated. A planner DVC grid structure with pore sizes of ~200, ~430 and ~520 μm was fabricated and its water-oil separation performance werewas evaluated. Despite theoretical calculations suggesting adequate water repelling pressures for pores around ~300 and ~360 μm, actual performance fell short due to defects from 3D printing and carbonization processes. A more robust design approach involves fabricating a cuboid shell-shaped VC grid structure with smaller pores (~150 μm), demonstrating continuous water-oil separation capabilities.

1. Introduction

Sea oil spill accidents do very harmful long-term damage to marine ecosystems [1]. In addition, large amounts of oil-mixed wastewater are generated in various industries such as mining, textiles, food, petrochemicals, and metal/steel industries, and cause environmental destruction [2]. An effective water-oil separation technology is important both for preventing ecological devastation and industrial purification. Among the various water-oil separation techniques, selective filtration or absorption using a porous structure is simple and cost-effective. In the selective filtration or absorption method, the surface wettability of porous structure is the key parameter for separation [3]. Since the hydrophobic porous structure can selectively block water and penetrate oil, various hydrophobic materials were applied to water-oil separation application.

A porous polypropylene (PP) material is commonly used as an oil absorber [4]. PP is a hydrophobic material, and a porous fiber structure can be obtained by melt blow method. The porous PP fiber sponge can absorb oil corresponding to 10 to 20 times the mass. Polydimethylsiloxane (PDMS), widely used for micro/nano replication process due to its hydrophobic surface and easy curing process, has also been applied to fabricate porous sponge structure by using sugar template [5] for oil absorption. Carbon materials including carbon nanotube [6] and reduced graphene oxide [7], also have hydrophobic property and have been used to realize porous sponge structure for oil absorption. A porous vitreous carbon (VC) structure fabricated by carbonization of thermoset polymer and sugar template mixture has also been proposed as a simple and low-cost approach for oil-water separation [8].

The water-oil separation performance was determined by the surface energy of the material and the geometrical properties of porous structure. However, most previous studies on the hydrophobic porous structure obtained the porous structure using a random fashion fabrication method and could not precisely control the geometrical properties of porous structure.

The 3-dimensional (3D) printing technique can be used to fabricate controllable micro-sized porous structures with artificial outer design. Shin et al. fabricated a cuboid shell shaped PDMS grid structure using a water-soluble 3D printed template and can increase oil absorbing capacity dramatically [9]. Niblett et al. fabricated a porous VC grid structure by carbonization of 3D printed UV-cured polymer grid structure for gas diffusion layer of a hydrogen fuel cell [10]. Since the direct carbonization of 3D printed parts is a simpler method to fabricate pore size controllable porous hydrophobic structure, in this study, we fabricated a VC grid structure by carbonization of digital light processing (DLP) 3D printed part for water-oil separation application.

The effects of pore size on the water-oil separation were experimentally evaluated and the theoretical model compared. In addition, a cuboid shell shape VC grid structure was fabricated and applied to continuous oil-water separation to confirm the insight of VC grid structure design and process development using the 3D printing technique.

2. Effects of pore size of VC grid structure on the water-oil separation

2.1 Experimental method and results

To realize a VC grid structure, the initial polymer grid structure was fabricated by a DLP 3D printer (Anycubic Photon M3 Max, Shenzhen Anycubic Technology Co., Ltd), and the fabricated 3D printed grid structure was carbonized at a maximum temperature of 1000 °C in a vacuum furnace [11-15]. Fig. 1(a) shows the 3D model of planner-type 4-layer grid structures with the definition of geometrical features, *p* and *d*. Fig. 1(b) shows the fabricated 3D printed 2-layer planner grid structure with an outer size of 60.5×60.5 mm^2, a pore size (*d*) of 1000 μm, and a pitch (*p*) of 1500 μm. The width of grid frame (*p*-*d*) was selected to 500 μm considering the stiffness of grid frame after carbonization. Fig. 1(c) shows the VC grid structure obtained by carbonization of the sample in Fig. 1(b). The outer size, pore size and pitch of VC grid structure were ~ 30×30 mm^2, ~430 μm, and a pitch (*p*) of ~660 μm. It clearly shows that the relatively large shrinkage (~56 %) occurred during the carbonization process due to thermal decomposition.

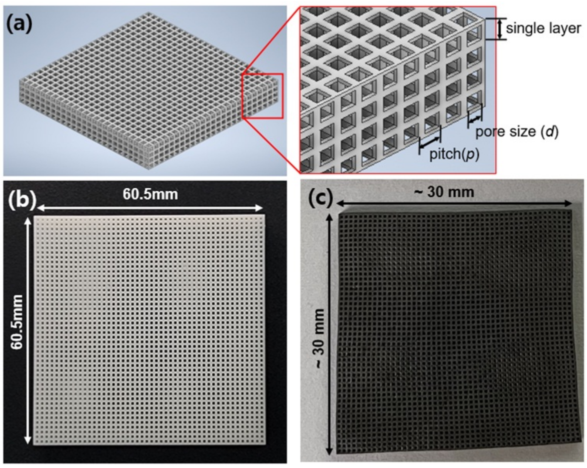

Fig. 1. (a) 3D model of planner type 4 layer grid structures; (b) 3D printed polymer grid structure with 4 layer; (c) carbonized VC grid structure with a pore size of 430 μm and a pitch of 660 μm.

To examine the effects of pore size of VC grid structure on the water-oil separation, we fabricated a planner VC grid structure with different pore sizes. Table 1 shows the summary of initial pore sizes, pitches, and shrinkage ratios of 3D printed polymer grid and carbonized VC gird structures. The same as the shrinkage ratio of the outer size the shrinkage ratio of pore size and pitch were also ~60 % because the shrinkage ratio was mainly affected by the thermal decomposition of the polymer material and the width of frame was the same in all samples.

To assess the water-oil separation efficiency based on the pore size of the VC grid structure, a straightforward experiment was devised and executed (Fig. 2(a)). A transparent acrylic cuboid vessel (80×40×40 mm³) with 20×20 mm² openings on both sides was utilized, with the fabricated planner VC grid

Table 1. Summary of pore sizes, pitches, and shrinkage ratios of 3D printed polymer grid and carbonized VC grid structures.

Sample		3D printed grid (μm)	VC grid (μm)	Shrinkage ratio (%)
Design#1 (500)	Pore size	500	~200	~60
	Pitch	1000	~400	~60
Design#2 (1000)	Pore size	1000	~430	~57
	Pitch	1500	~660	~56
Design#3 (1250)	Pore size	1250	~520	~58
	Pitch	1750	~740	~58

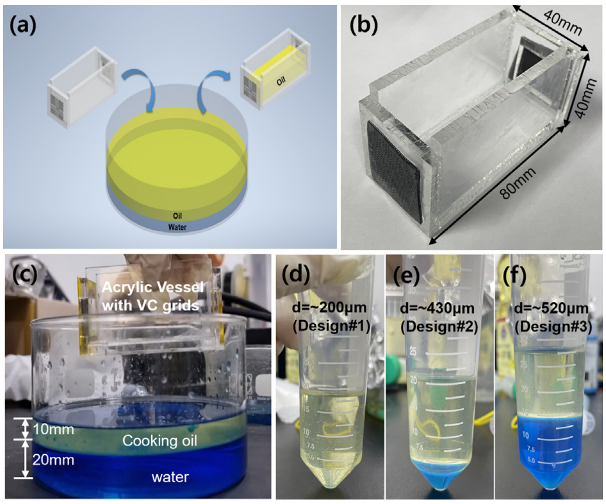

Fig. 2. Experimental setup for assessing the water-oil separation performance of planner VC grid structures with varying pore sizes: (a) schematic of the experiment; (b) image of the transparent acrylic cuboid vessel with 20×20 mm² openings blocked by planner VC grid structures; (c) depiction of the vessel immersed in the water-oil mixture; images showing the liquid collected by the vessel with VC grid structures of different pore sizes: (d) ~200 μm; (e) ~430 μm; (f) ~520 μm.

structures affixed to block these openings (Fig. 2(b)). Subsequently, the vessel containing the VC grid structures was submerged into a beaker containing a mixture of water and cooking oil (20 mm water layer and 10 mm oil layer) (Fig. 2(c)). Following a 30-second immersion, the collected liquid was promptly transferred into 50 ml conical tubes. The liquid collected by the vessel with VC grid structures of varying pore sizes is depicted in Figs. 2(d)-(f). With increasing pore size, a greater volume of liquid was amassed due to the consistent frame width of the VC grid structure. The percentage of cooking oil in the total collected liquid was measured at 99 %, 45.5 %, and 35.3 % for pore sizes of approximately 200 μm, 430 μm, and 520 μm, respectively. This indicates the suitability of a pore size around 200 μm for water-oil separation applications.

2.2 Theoretical analysis

The phenomenon in which water does not selectively permeate through a porous hydrophobic surface occurs because the repel pressure due to the surface tension of water, explained by the Young−Laplace equation, is greater than the pressure of water existing outside. The repel pressure due to the surface tension of water according to pore size (d) is calculated as Eq. (1) [16].

$$P_{rep} = -\frac{4\gamma_{wo}\cos\theta_{wo}}{d} \tag{1}$$

where P_{rep} is the water repel pressure at the porous hydrophobic structure, γ_{wo} is the interfacial tension of an water-oil interface (30.26 mN/m) [17], θ_{wo} (148.3°) is the contact angle of water at oil environment on the smooth VC surface as shown in Fig. 3. In the experiment in Sec. 2.1, the maximum pressure of water applied to the opening of the vessel is calculated as Eq. (2).

$$P_{max} = \rho_o g h_o + \rho_w g h_w \tag{2}$$

where P_{max} is the maximum water pressure, ρ_o is the density of oil (895 kg/m^3), ρ_w is the density of water (997 kg/m^3), h_o is the initial height of oil layer (10 mm) and h_w is the initial height of water layer at the bottom of opening of the vessel (10 mm), and g is the gravity acceleration (9.81 m/s^2). The calculated P_{max} is 185.6 N/m^2.

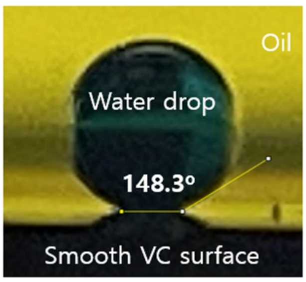

Fig. 3. Contact angle of water at oil environment on the smooth VC surface.

To calculate the water repel pressure of the fabricated VC grid structure with different pore sizes, the pore sizes of VC grid structures were measured as shown in Fig. 4. The measured pore sizes are ~200, ~430 and ~520 μm as. The water repel pressure of each different pore size VC grid structure can be calculated by Eq. (1) and the calculated water repel pressures were 514.91, 239.49, and 198.04 N/m^2 for the VC grid structures with pore sizes of ~200, ~430 and ~520 μm, respectively. Although the calculated water repel pressures are higher than the maximum water pressure (185.6 N/m^2) for all fabricated VC grid structures, the VC grid structures with pore sizes of ~430 and ~520 μm did not block the penetration of water in the experiments. It might be due to the imperfection of DLP 3D printed parts and warpage and breakage of the grid frame structure during the carbonization process. Therefore, a more robust design of pore size is required for the VC grid structure fabricated by carbonization of 3D printed part for water-oil separation application.

3. Demonstration of continuous water-oil separation using cuboid shell shape VC grid structure and oil suction system

To demonstrate a continuous water-oil separation using a VC grid structure, a cuboid shell shape VC grid structure with a perforated top was fabricated as shown in Fig. 5. The initial

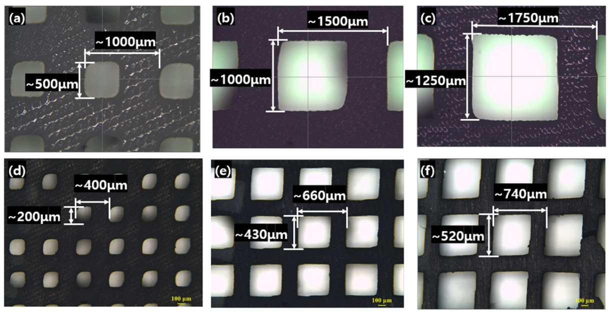

Fig. 4. Pore size of 3D printed structure: (a) design#1; (b) design#2; (c) design#3; pore size of VC grid structure: (d) design#1; (e) design#2; (f) design#3.

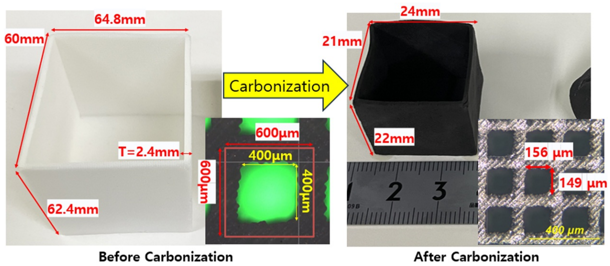

Fig. 5. Fabrication of cuboid shell shape VC grid structure VC grid structure for continuous water-oil separation.

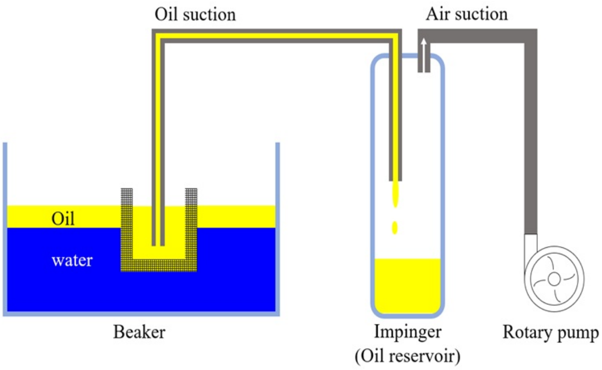

Fig. 6. Schematics of continuous water-oil separation test system.

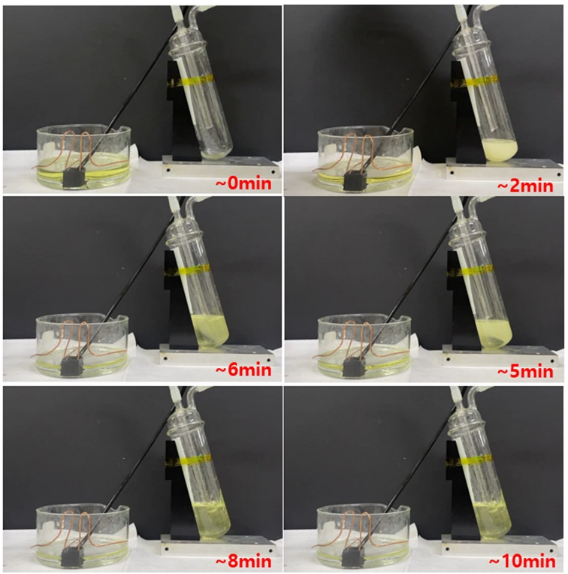

Fig. 7. Time series pictures of a continuous water-oil separation experiment.

outer size of the cuboid shell shape 3D printed grid structure was 64.8×60×62.4 mm^3 and the outer size of the VC grid structure was ~ 24×21×22 mm^3. Based on the robust design concept, the initial pore size of 3D printed grid structure of 400 μm was selected. The initial frame width of 3D printed grid structure of 200 μm was selected to increase the pore ratio of the grid structure. The pore size and pitch of the carbonized VC grid structure were ~150 μm and ~210 μm, respectively. The calculated shrinkage ratio was ~63 %, and it is slightly higher than the planner VC grid structure (~60 %) explained in Sec. 2.1. The shrinkage ratio in the carbonization process of the smaller feature is higher than the larger feature because the shrinkage ratio of polymer material during the carbonization is anisotropic and the shrinkage ratio is gradually decreased from the surface to inside [18, 19].

The continuous water-oil separation experimental setup was designed and constructed by connecting a cuboid shell shape carbon grid structure to an impinger and a rotary pump using a rubber tube as shown in Fig. 6. An oil spill situation was assumed by filling a beaker with a solution mixed with 230 ml of water and 230 ml of cooking oil. A rotary pump was used to create a pressure state lower than atmospheric pressure inside the impinger, and the oil collected into the cuboid shell shape VC grid structure was charged inside the impinger using the pressure difference. Fig. 7 shows the time series pictures of a continuous water-oil separation experiment. It was confirmed that the cuboid shell shape VC grid structure with a pore size of ~150 μm inside the beaker containing the water-oil mixture selectively penetrates only cooking oil from the mixture. After 8 minutes of starting oil separation, the oil capacity inside the impinger did not increase, and it can be confirmed that most of the oil in the water-oil mixture was separated. The water-oil separation efficiency of the cuboid shell shape VC grid structure manufactured with an oil ratio inside the impinger of over 99 % was verified. Under experimental conditions, the oil separation speed was measured to be ~30 ml/min.

4. Conclusions

As a potential application of the 3D printing technique, a VC grid structure for water-oil separation was investigated. Planner VC grid structures with different pore sizes were fabricated and their water-oil separation performances were evaluated. Although the theoretical water repel pressures for the pore sizes of ~430 and ~500 μm were higher than the outer water pressure in the experiment, the VC grid structure with the pore sizes of ~430 and ~500 μm did not show perfect water-oil separation performance, due to the defects occurring in both 3D printing and carbonization process. As a robust design concept, a cuboid shell shape VC grid structure with a pore size of ~150 μm was fabricated and its continuous water-oil separation performance was demonstrated. Although the cuboid shape VC grid structure can perfectly separate oil from the water-oil mixture, the speed of ~ 30 ml/min is relatively slow for commercial applications. Therefore, an optimization of the DLP 3D printing process and carbonization process to minimize the defects of grid structure with micro-sized pores, and the optimization of pore size to perfectly separate water-oil mixture and maximize separation speed are needed. In addition, a zig-zag shell shape VC grid structure also can be realized by 3D printing and carbonization methods and it can improve the separation speed due to the increase of contact areas of the water-oil mixture. The optimizations of process, pore size and outer shape of VC grid structure to meet the commercial use requirements are the subject of our ongoing research.

Acknowledgments

This research was supported by the Chung-Ang University Research Grants in 2021, and by the National Research Foundation of Korea (NRF) grant funded by the Korea government (MSIT) (No. 2021R1A2C2004458).

Nomenclature

p : Pitch
d : Pore size
P_{rep} : Water repel pressure
γ_{wo} : Interfacial tension of an water-oil interface
θ_{wo} : Contact angle of water at oil environment
P_{max} : Maximum water pressure
ρ_o : Density of oil
ρ_w : Density of water
h_o : Initial height of oil layer
h_w : Initial height of water at the bottom of opening

References

[1] I. Leifer, W. J. Lehr, D. Simecek-Beatty, E. Bradley, R. Clark, P. Dennison, Y. Hu, S. Matheson, C. E. Jones, B. Holt, M. Reif, D. A. Roberts, J. Svejkovsky, G. Swayze and J. Wozencraft, State of the art satellite and airborne marine oil spill remote sensing: application to the BP deepwater horizon oil spill, *Remote Sensing of Environment*, 124 (2012) 185-209.
[2] S. Rasouli, N. Rezaei, H. Hamedi, S. Zendehboudi and X. Duan, Superhydrophobic and superoleophilic membranes for oil-water separation application: a comprehensive review, *Materials & Design*, 204 (2021) 109599.
[3] N. Zhang, Y. Qi, Y. Zhang, J. Luo, P. Cui and W. Jiang, A review on oil/water mixture separation material, *Industrial & Engineering Chemistry Research*, 59 (33) (2020) 14546-14568.
[4] Z. Zhang, D. Yu, X. Xu, H. Li, T. Mao, C. Zheng, J. Huang, H. Yang, Z. Niu and X. Wu, A polypropylene melt-blown strategy for the facile and efficient membrane separation of oil-water mixtures, *Chinese J. of Chemical Engineering*, 29 (2021) 383-390.
[5] S. Choi, T. Kwon, H. Im, D. Moon, D. J. Baek, M. Seol, J. P. Duarte and Y. Choi, Polydimethylsiloxane (PDMS) sponge for the selective absorption of oil from water, *ACS Applied Materials & Interfaces*, 3 (12) (2011) 4552-4556.
[6] X. Gui, H. Li, K. Wang, J. Wei, Y. Jia, Z. Li, L. Fan, A. Cao, H. Zhu and D. Wu, Recyclable carbon nanotube sponges for oil absorption, *Acta Materialia*, 5912 (2011) 4798-4804.
[7] Y. He, Y. Liu, T. Wu, J. Ma, X. Wang, Q. Gong, W. Kong, F. Xing, Y. Liu and J. Gao, An environmentally friendly method for the fabrication of reduced graphene oxide foam with a super oil absorption capacity, *J. of Hazardous Materials*, 260 (2013) 796-805.
[8] M. A. Asgar, J. Kim, J. W. Yeom, S. Lee, M. R. Haq and S. Kim, Facile fabrication of microporous vitreous carbon for oil/organic solvent absorption, *Environmental Technology & Innovation*, 24 (2021) 101946.
[9] J. H. Shin, J. H. Heo, S. Jeon, J. H. Park, S. Kim and H. W. Kang, Bio-inspired hol-low PDMS sponge for enhanced oil-water separation, *J. of Hazardous Materials*, 365 (2019) 494-501.
[10] D. Niblett, Z. Guo, S. Holmes, V. Niasar and R. Prosser, Utilization of 3D printed carbon gas diffusion layers in polymer electrolyte membrane fuel cells, *International J. of Hydrogen Energy*, 47 (55) (2022) 23393-23410.
[11] J. Ju, S. Lim, S. Kim and J. Seok, A method to fabricate a low-cost, large-area vitreous carbon mold for glass molded microstructures, *International J. of Precision Engineering and Manufacturing*, 16 (2015) 287-291.
[12] M. R. Haq, Y. K. Kim, J. Kim, J. Ju and S. Kim, Fabrication of all glass microfluidic device with superior chemical and mechanical resistances by glass molding with vitreous carbon mold, *Journal of Micromechanics and Microengineering*, 29 (7) (2019) 075010.
[13] J. Kim, D. Hong, M. A. Badshah, X. Lu, Y. K. Kim and S. Kim, Direct metal forming of a microdome structure with a glassy carbon mold for enhanced boiling heat transfer, *Micromachines*, 9 (8) (2018) 376.
[14] H. Jang, M. R. Haq, Y. Kim, J. Kim, P. Oh, J. Ju, S. M. Kim and J. Lim, Fabrication of glass microchannel via glass imprinting using a vitreous carbon stamp for flow focusing droplet generator, *Sensors*, 18 (1) (2017) 83.
[15] M. A. Badshah, J. Kim, J. Yeom, N. Abbas, M. R. Haq, Y. Kim, X. Lu and S. Kim, Glass nanoimprinted plasmonic nanostructure for high power laser stable surface-enhanced Raman spectroscopy substrate, *Applied Surface Science*, 542 (2021) 148587.
[16] C. Chen, D. Weng, A. Mahmood, S. Chen and J. Wang, Separation mechanism and construction of surfaces with special wettability for oil/water separation, ACS *Applied Materials & Interfaces*, 11 (11) (2019) 11006-11027.
[17] Y. Cong, W. Zhang, C. Liu and F. Huang, Composition and oil-water interfacial tension studies in different vegetable oils, *Food Biophysics*, 15 (2020) 229-239.
[18] M. A. Gondal, M. S. Sadullah, M. A. Dastageer, G. H. McKinley, D. Panchanathan and K. K. Varanasi, Study of factors governing oil–water separation process using TiO_2 films prepared by spray deposition of nanoparticle dispersions, *ACS Applied Materials & Interfaces*, 6 (16) (2014) 13422-13429.
[19] M. R. Haq, J. Kim, J. Ju, Y. K. Kim, W. J. Chang and S. Kim, Development of shrinkage model of micro structured vitreous carbon mold for glass molding, *J. of Mechanical Science and Technology*, 33 (12) (2019) 5747-5752.

Ju Wan Kim received his B.S in 2023 in Mechanical Engineering at Chung-Ang University, Seoul, Republic of Korea. He is currently pursuing the M.S. in Department of Mechanical Engineering, Chung-Ang University, Seoul, Republic of Korea. His research interests include micro/nano-scaled metal structuring and design and fabrication of micro/nano structure using a carbonized vitreous carbon materials.

Chanwoo Kim received his B.S. in 2024 in Mechanical Engineering at Chung-Ang University, Seoul, Republic of Korea. His research interests include 3D printing and its applications.

Hyunjin Na received her B.S. in 2024 from the School of Mechanical Engineering at Chung-Ang University, Seoul, Republic of Korea. Her research interest includes 3D printing and its applications.

Seongmin Lee received his M.S. in 2020 from the Department of Mechanical System Engineering at Chung-Ang University, Seoul, Republic of Korea. He is currently pursuing a Ph.D. in Mechanical Engineering, Chung-Ang University, Seoul, Republic of Korea. His research interests include design and fabrication of micro/nanostructures for optical biosensors, LED lighting, and fuel cell carbon support components.

Seongyong Byun received his M.S. in 2024 in Mechanical Engineering at Chung-Ang University, Seoul, Republic of Korea. His research interests include design and fabrication of micro/nano scaled metal structuring and NOx/SOx monitoring system.

Suyeon Seok received her B.S. in 2023 in Mechanical & Design Engineering at Hongik University, Sejong, Republic of Korea. She is currently pursuing an M.S. at the Department of Mechanical Engineering, Chung-Ang University, Seoul, Republic of Korea. Her research interests include fabrication of micro/nano structured glass molded components.

Young Kyu Kim received his Ph.D. in 2019 in Mechanical Engineering at Chung-Ang University, Seoul, Republic of Korea. He is currently a Research Professor in the Department of Computer Science and Engineering at Chung-Ang University, Seoul, Republic of Korea. His research interests include design and fabrication of micro/nano structured devices using a carbonized vitreous carbon materials.

Seok-min Kim received his Ph.D. in 2007 in Mechanical Engineering at Yonsei University, Seoul, Republic of Korea. He is currently a Professor in Mechanical Engineering at Chung-Ang University, Seoul. His current research interests include design and fabrication of micro/nanostructures for optical biosensors, micro fluidic chips, concentrator photovoltaic system, digital display, LED lighting, and enhanced boiling heat transfer surface.